Chapter 5
Evolution of Some Cephalopods During Major Extinctions

5.1 Repetition of Lineages by Retrograde Evolutionary Jumps in Ammonites

Iterative evolution is the most striking property of the ammonoid distribution during their long life. The very large scale phylogeny of the three major distinct groups occurring during the Paleozoic and the Mesozoic periods is shown in Fig. 5.1 which demonstrates that major evolutionary jumps in ammonoids occur during severe extinction events. These are characterized by the rapid appearance of simple, primitive-looking forms which are similar to remote ancestors of their more complex immediate progenitors. Such forms are often atavistic and homeomorphic species generated during such sublethal stress events and they can be separated by several millions of years from their initial ancestor. A striking example of such an iteration is given in Fig. 5.2 presenting the very simple morphology of the smooth evolute (or *Xenodiscus* group in a larger sense), appearing at the Permian Triassic boundary and giving rise to all the ammonoids known as Ceratitina. The group is affected by a quasi extinction at the Triassic Jurassic boundary and its recovery starts from the equally simple smooth evolute *Psiloceras*, which are, in turn, quasi homeomorph of *Ophiceras*. These two primitive forms developed phyletic lineages with many common features (Fig. 5.2), even though *Psiloceras* is derived from *Ophiceras* through a long and complex series of successive and distinct lineages. The detail of the relation between Phylloceratina and Psiloceras is given in Fig. 5.3.

J. Guex, *Retrograde Evolution During Major Extinction Crises*, SpringerBriefs in Evolutionary Biology, DOI 10.1007/978-3-319-27917-6_5

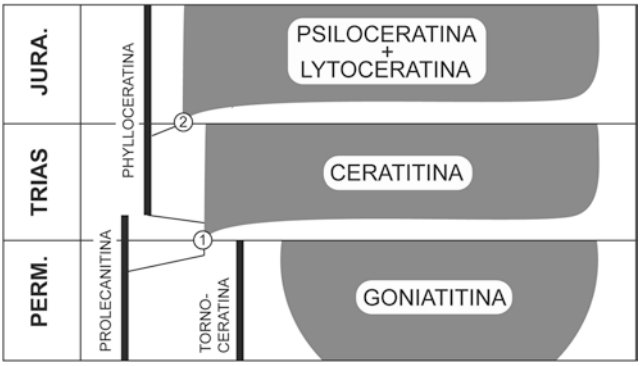

Fig. 5.1 Large scale evolution of the different suborders of ammonoids. (1) Ophiceras, (2) Psiloceras (see text and Sect. 2.2). From Guex (2006)

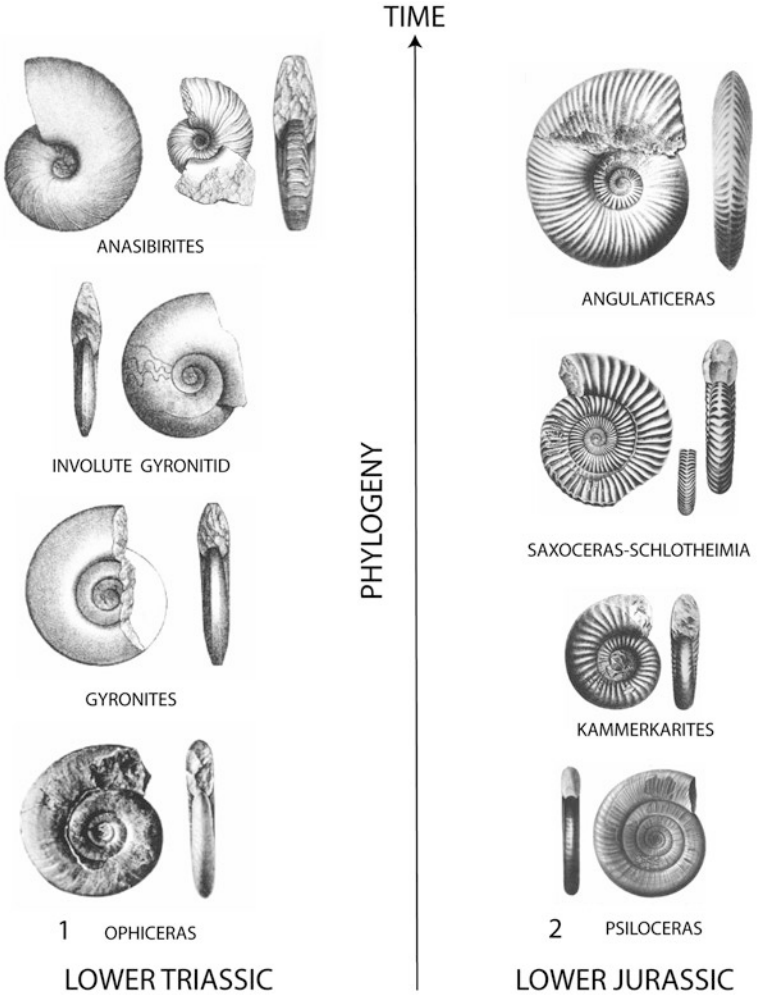

Fig. 5.2 Evolution of the earliest Ceratitina and Psiloceratina at the base of the Triassic and of the Jurassic. From Guex (2006)

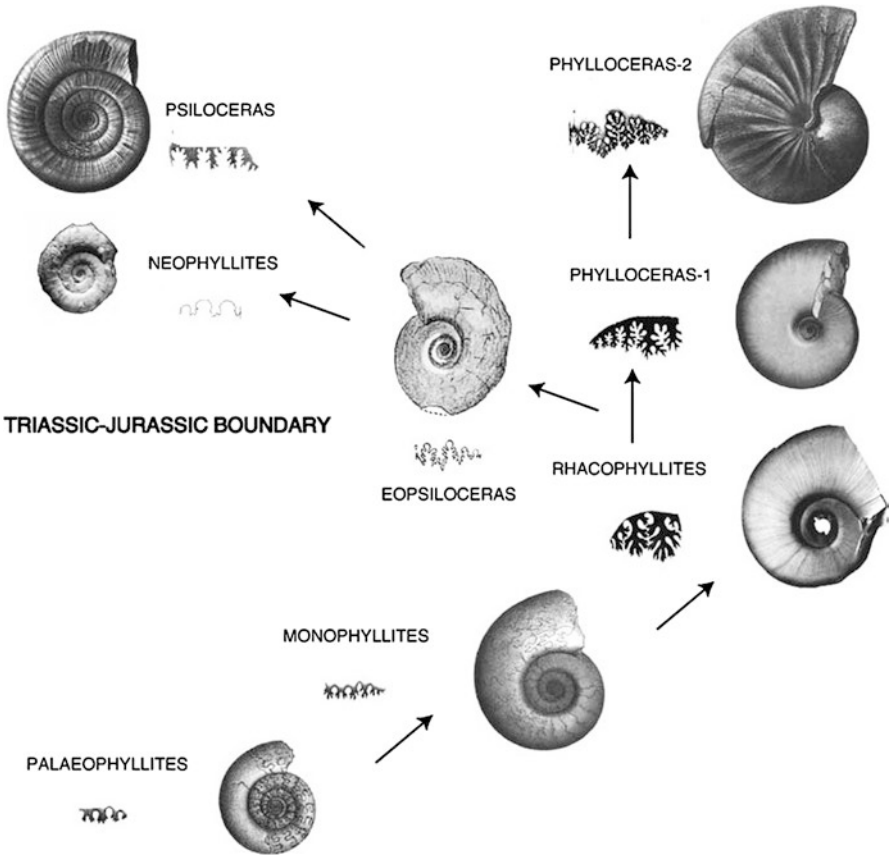

Fig. 5.3 Details of the relations between the Phylloceratida and Psiloceras (from Guex 2006). See Sect. 2.2 and Fig. 5.1

5.2 Evolutionary Jumps of the Ammonites During the Middle-Late Toarcian Crisis

Here we return to two examples which we consider particularly illustrative (loc. cit.). The first concerns the evolution of the Middle Toarcian *Paronychoceras* (the microconchs of *Phymatoceras*, see Guex 2000) and of their Late Toarcian offshoots, *Onychoceras* (the microconchs of *Hammatoceras*) (Fig. 5.4). The oldest known *Paronychoceras*, *P. pseudoplanum*, is a tiny relatively evolute smooth form with no keel or sign of ribbing. It is followed by *P. costatum*, which has no keel but faint crescentic lateral ribs. Its direct offshoot is represented by *Pseudobrodieia lehmanni*, itself followed by *Brodieia* sp. n. ind. which is ribbed, keeled and has lateral lappets. In the Early Late Toarcian (uppermost Variabilise zone-Thouarsense zone) the first microconch lineage gives rise to *Onychoceras planum*, followed by

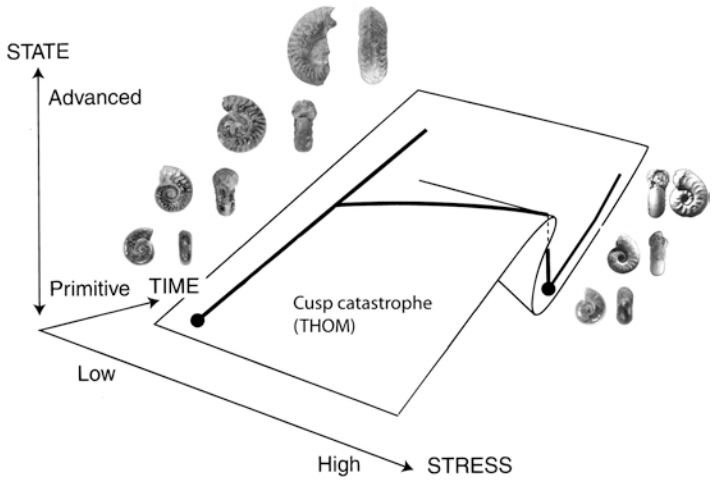

Fig. 5.4 Evolution of the *Paronychoceras* → *Pseudobrodieia* → *Brodieia* lineage and catastrophic repetition of the early part of the lineage at the Middle-Late Toarcian boundary (from Guex 2001)

O. tenue (Early Insigne Zone) and *O. differens* (Late Insigne Zone). It is of importance that no intermediate forms linking the two successive lineages are known (Fig. 5.4). This possibly reflected the poor preservation of this group during the Middle-Late Toarcian crisis.

A second lineage of interest is observed during the same time which shows a similar case of iterative evolution: the *Hildaites* → *Phymatoceras* → *Haugia* → *Denckmannia* (Middle Toarcian Phymatoceratinae) which gives rise to the plexus *Podagrosites* → *Pseudogrammoceras* → *Phlyseogrammoceras* → *Huddlestonia* lineage (Upper Toarcian Grammoceratidae). The evolution of the Phymatoceratinae and one of their derivatives, the Grammoceratidae, is illustrated in Fig. 5.5. This lineage is rooted in evolute forms of the Lower Toarcian which belong to the genus *Hildaites*, and which evolved into the involute group of *Haugia* via *Phymatoceras*. During the Late-Middle Toarcian, the variability of *Haugia* increased and this group gave rise to a relatively evolute form called *Denckmannia* which, in turn, gave rise to a very evolute and simply ribbed ammonite, *Podagrosites*. This new group is a perfect homeomorph of the ancestral *Hildaites*. Starting from the *Podagrosites* pole, we observe a continuous morphological transition towards the different species of *Pseudogrammoceras,* eventually giving rise to the involute and fasciculate *Phlyseogrammoceras* and to the smooth oxycone *Hudlestonia*. This example demonstrates that the transition from involute forms (which are the outcome of a major evolutionary trend) towards a primitive looking evolute form is achieved through an increase of the variability of the ancestral advanced group during an episode of stress. It should be noted that such a transformation is global (i.e. it affects the whole ontogeny) and does not result from a simple heterochrony such as neoteny or progenesis.

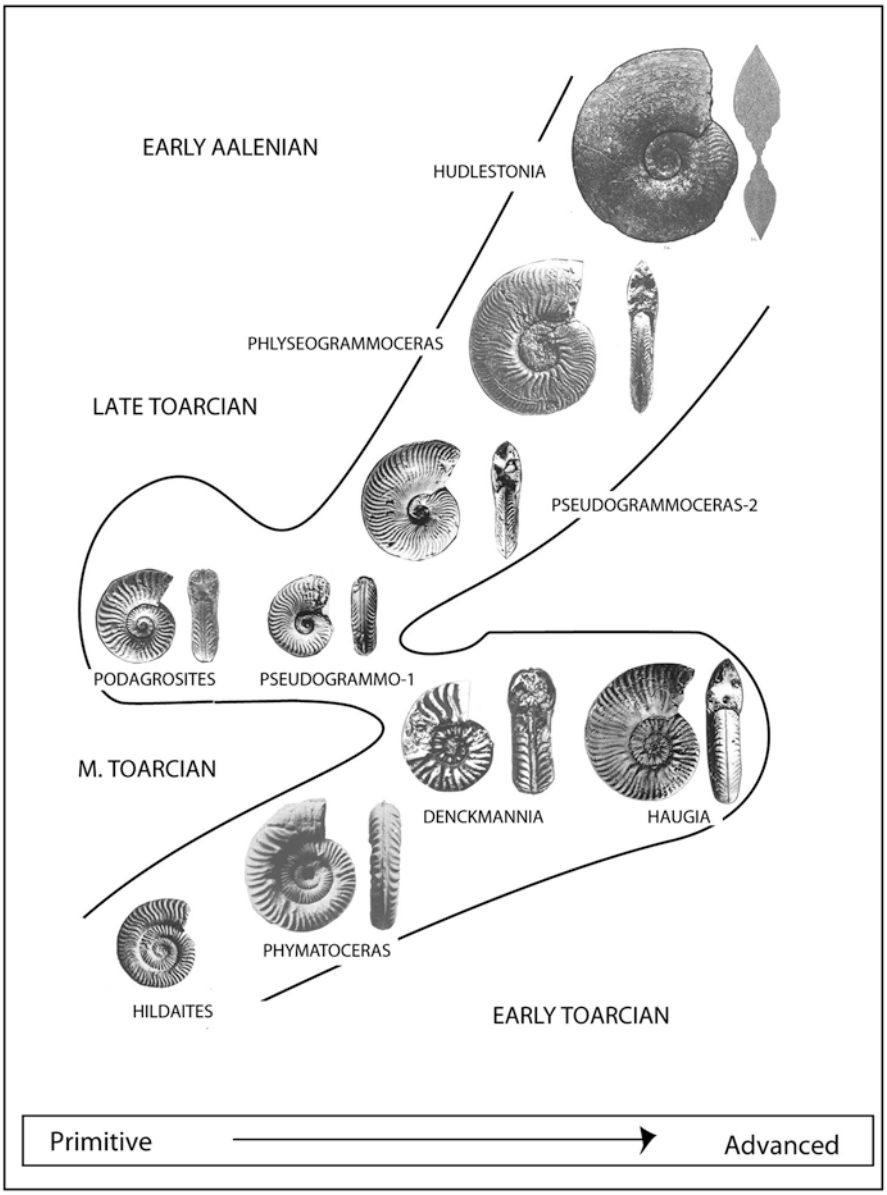

Fig. 5.5 Anagenetic evolution of the *Hildaites* → *Phymatoceras* → *Haugia* lineage and catastrophic appearance of the sub-homeomorphic *Podagrosites* → *Pseudogrammoceras* → *Phylseogra mmoceras* lineage (from Guex 2001)

5.3 Retrograde Covariation During Extinction Episodes

5.3.1 Buckman's First Law of Covariation

The *Buckman's First Law of covariation* named so by Westermann (1966) following the first observations by Buckman (1887) in *Sonninia* and *Amaltheus* was originally described as follows: "Roughly speaking, inclusion and compression of the whorls correlate with the amount of ornament—the most ornate species being the more evolute (i.e. loosely coiled) and having almost circular whorls…" (Buckman 1887).

Some Pliensbachian ammonites belonging to the genus *Amaltheus* provide probably the best example of covariation. In this group, more specifically in the *A. gibbosus* group, all transitions between evolute and strongly spinose forms and quasi-smooth involute forms at the other extreme are observed (Figs. 5.6 and 5.11b), excluding the possibility to explain this compelling variability as a special case of scale and proportionality (Hammer and Bucher 2005).

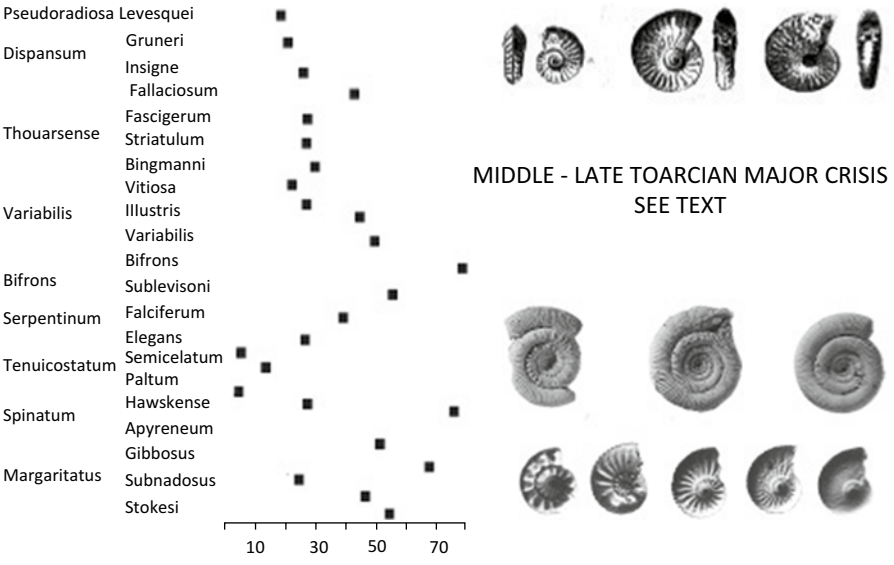

Fig. 5.6 Examples of covariation during the unstable Pliensbachian-Toarcian period: Correlation between the development of extreme retrograde polymorphism and main extinction events (see variations of the species richness). Margaritatus zone: *Amaltheus gibbosus*. Tenuicostatum Zone: *Dactylioceras clevelandicum* (courtesy of Mike Howarth). Dispansum Zone: *Osperleioceras reynesi*

5.3.2 *The Case of* Osperleioceras reynesi

As already seen above, the crisis periods are not favourable to fossilization. During such perturbated intervals, the fossils are absent, rare or badly preserved. However, during the Middle Upper Toarcian crisis, the genus *Osperleioceras* is very well recorded in the Causses Basin (Southern France) and we can follow precisely the genesis of the loosely coiled and atavistic *Osperleioceras reynesi* from its tightly coiled ancestor *O. bicarinatum* which itself derived from the common ancestor Harpoceras.

The details of that very important morphological genesis of a primitive looking form are illustrated in Fig. 5.7. Note that the last step of that evolution is marked by a clear phenomenon of covariation, discussed below.

5.3.3 *A Morphogenetic Explanation of Buckman's Covariation*

Covariation depends on the internal shell geometry, namely the lateral and ventral curvature of the shell which controls the amount of morphogens present in the more or less curved mantle, the most salient ornamentation being present where the whorls are most curved, shells with slight angular bulges often being spinose or carinate and flat ones being almost smooth (Guex 1999, p 42). The empirical conclusion was that the covariation phenomenon could be explained within the framework of Gierer-Meinhardt's reaction diffusion models. To prove that conclusion, André Koch simulated the distribution of "morphogens" (in the physical sense) in a quadrangular body chamber and demonstrated that morphogens maxima are located, as expected, in the part of the mantle located in the angular parts of the shell.

For this, Andre Koch (in Guex et al. 2003) calculated a numerical solution of the Gierer-Meinhardt equations for a cross section through an ammonite shell, orthogonal to the growth axis. The solution of the standard reaction-diffusion equations of Gierer-Meinhardt in a bidimensional domain is as follows:

$$\partial_t a = D_a \Delta a + \rho_a a^2 / h - \mu_a a + \sigma_a$$

$$\partial_t h = D_h \mathrm{Dh} + \rho_h a^2 - \mu_h h$$

with $\Delta \equiv \partial^2 / \partial_x{}^2 + \partial^2 / \partial_y{}^2; a(x,t)$ and h(x,t) corresponding to the activator and inhibitor morphogens, respectively. In the numerical simulation, the constants have the following values:

$$D_a = 0.012 \quad \rho_a = 1.0\, \mu_a = 0.01 \quad \sigma_a = 0.002$$

$$D_h = 0.4 \rho_h = 1.0 \mu_h = 0.01$$

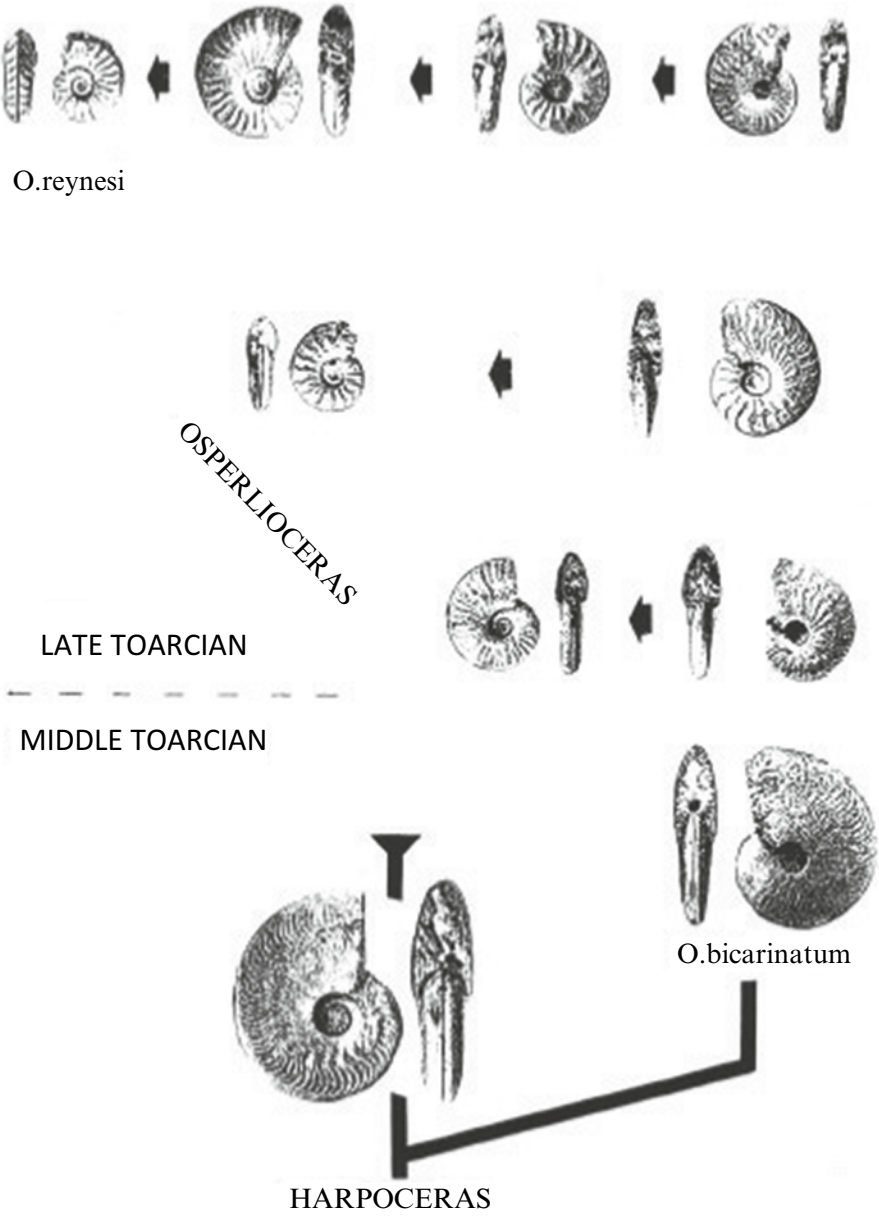

Fig. 5.7 Evolution of *Osperleioceras* through the Middle-Late and Late Toarcian crises, showing the development of a retrograde polymorphism in the Reynesi subzone. From Guex (1992)

The units of distance, time and concentration are arbitrary! The domain of computation corresponds to the union of the two following areas:

1. Area delimited by two arcs of circles {(−33.5120,−12.1072), 50.00} and {(−24.5332, −11.5931), 40.00}, and contained in the region $x \geq 0$ and $y \geq -0.052$.
2. Area delimited by two arcs of circles {(33.5120, −12.1072), 50.00} and {(24.5332, −11.5931), 40.00}, and contained in the region $x \leq 0$ and $y \geq -0.052$.

The boundaries of the domains are supposed to be impervious for the inhibitor. The outer boundary (arc of circle of radius 50.00) is unaffected by the activator whereas the other boundaries are susceptible to this factor. The choice of these boundary conditions is motivated by the following arguments: The activator is supposed to diffuse freely outside the mantle's cells into the environment (intercellular medium and sea water).

The reaction-diffusion equations are solved numerically on a hexagonal mesh containing 1500 nodes corresponding to a hexagon radius of 0.23 units. The concentrations $a(x,t)$ and $h(x,t)$ are determined at each node of the mesh. The initial values of the concentrations at $t=0$ correspond approximatively to the values taken from the (unstable!) homogenous stationary solution. We add small random deviations ε(x,0) to the concentrations of the activator to allow the system to leave the initially homogenous state. The initial values are thus given by:

$$a(x,0) = 1.0\left[1 + \varepsilon(x,0)\right] \quad \text{with} \quad -0.05 < e(x,0) < +0.05$$

$$h(x,0) = 100.0.$$

The stationary inhomogeneous solution is found using a standard iterative procedure (details in Guex et al. 2003). Similar conclusions were obtained by Newell et al. (2008) in their general study of phyllotaxy: "… buckling leads to a template for primordia, it is growth that leads to the visible primordial bumps and phylla. This growth is postulated to be a biochemical response, perhaps through chemical agents such as auxin, to the local stress or curvature inhomogeneities of the buckled surface …". In our carbonate shelly invertebrates, the morphogens have obviously nothing to do with auxin but could simply be Ca^{2+} ions.

The output of Koch's calculation is given in Fig. 5.8, showing the distribution of the activator and inhibitor in a bended shell: very low concentration in the smooth part and very high concentration in the curved part.

More recently, an alternative model leading to the same kind of conclusions has been proposed by Mercker et al. 2013 where the authors write that "biomechanical forces may replace the elusive long-range inhibitor and lead to formation of stable spatially heterogeneous structures without existence of chemical prepatterns. We propose new experimental approaches to decisively test our central hypothesis that *tissue curvature and morphogen expression are coupled in a positive feedback loop"*.

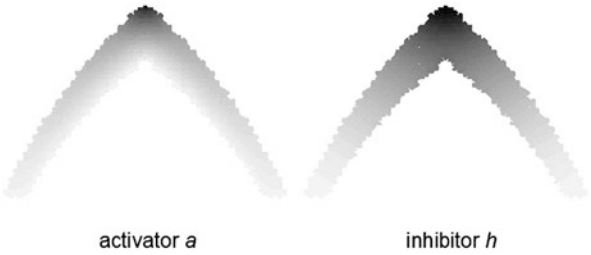

Fig. 5.8 Output of Koch's program showing the relative concentration (*white to dark grey*) of the activator and inhibitor in the bended shell (see text). From Guex et al. (2003)

It might be useful to note that a multitude of mathematical models can simulate the pattern formation in shelly organisms. To illustrate this we can mention the fact that phyllotaxy, a domain studied by botanists, has been formally described by models developed in three totally different fields of mathematics: pure geometry by Van Iterson (1907), pure physics by Douady and Couder (1992) and reaction-diffusion by Meinhardt et al. (1998). In other words it is clear that our model of spine formation in ammonites (Fig. 5.8) is obviously not the only possible, even if it has nothing to do with a proportionality problem.

5.3.4 Covariation and Environmental Stress

One notable characteristic of covariation in Buckman's sense is that it usually generates extreme morphotypes of atavistic habitus with simple and evolute morphologies and it seems to occur exclusively during episodes of environmental stress.

To demonstrate this we shall stay in the upper part of the Lower Jurassic (Late Pliensbachian-Toarcian), a period of high ecological instability that provides evidence of some of the best documented extinction events in ammonoid history.

The variations in ammonite biodiversity, expressed as species richness, from the Pliensbachian-Toarcian boundary up to the lower part of the Late Toarcian (Dera et al. 2010) are correlated with the standard ammonite biochronological scale (Fig. 5.6).

The first extinction event is placed at the transition between the Gibbosus and Spinatum zones in the Late Pliensbachian (Meister 1988, 1989; Meister and Stampfli 2000; see also Dera et al. 2010). The evolute spinose zonal index *Amaltheus gibbosus* is an atavistic form generated from involute *A. margaritatus* which strongly resembles the ancestral morphology of the Sinemurian *Eoderoceras* (Guex et al. 2003, and see Fig. 5.11).

Across the Pliensbachian-Toarcian boundary (Fig. 5.6) the Dactylioceratidae reacted similar to other groups by a marked increase in variability with extreme forms leading from the depressed and strongly spinose *Dactylioceras crosbeyi* group to serpenticone forms with simple ornamentation of the *Eodactylites* morphogroup, another typical case of covariation.

The next crisis, known as the Early Toarcian Oceanic Anoxic Event, is characterized by the occurrence of the same kind of variability increase within the *Dactylioceras semicelatum* and *D. clevelandicum* group which develops spinose forms with cadicone internal whorls (Howarth 1973). This episode is also characterized by the appearance of evolute Hildoceratids known as *Hildaites*, derived from the relatively involute Protogrammoceratids. In this latter case the complete transition between the two groups is not well recorded.

During the Middle-Late Toarcian transition, an exceedingly important faunal turnover is observed with the disappearance of the Hildoceratids, Dactylioceratids and Phymatoceratids which are replaced in the ammonite populations by the Hammatoceratids and Grammoceratids. This crisis, like the others, is marked by a strong increase in polymorphism of the ammonites and is also marked by the appearance of atavistic/evolute primitive looking ammonites such as *Podagrosites* generated by *Pseudogrammoceras* (see above), which are similar to the ancestral lower Pliensbachian *Fuciniceras* (Guex 1992, 2006).

The same kind of biotic situation occurs once more during the Late Insigne–Early Levesquei crises (Guex 1975; Dera et al. 2010) where the disappearance of abundant *Osperleioceras*, most typical Hammatoceratids, *Alocolytoceras, Buckmanites* and *Oxyparoniceras* is observed. In the topmost abundantly fossiliferous beds of the Late Insigne Zone (Dispansum subzone) a huge polymorphism is observed again in the *Osperleioceras reynesi* group with typical *Osperleioceras* like *O. alterans-wunstorfi* (Guex 1975, Pl. 8, Fig. 3) giving rise to simplified *O. reynesi* (Guex 1975, Pl. 8, Fig. 2), a form characterized by an evolute coiling and simple, strong and almost straight lateral ribs (Guex 1992, Fig. 4; Morard and Guex 2003, Fig. 1). The same is detected in *Hammatoceras* of the *bonarellii* group (Guex 1975, Pl. 9, Fig. 12) which gives rise to serpenticone *Catulloceras* (Guex 1975, Pl.2, Fig. 4), the direct ancestor of the *Dumortieria* and *Pleydellia* leading to all the Haploceratacea of the Middle and Upper Jurassic (Guex 1992, Fig. 5). Other examples of atavisms occurring during high environmental stress are discussed and illustrated in Guex (2006).

5.3.5 Ecophenotypes and Stress in Benthic Foraminifera

Benthic foraminifera are well known to be extremely sensitive to environmental stress (Camacho et al. 2015; Barras et al. 2010) and several classical studies have shown that the variability of these organisms was polarized in function of such perturbations. That polarization is mainly characterized by a differential colonization of the ecological niches where the geometrically simplest and archaic forms are more frequent in unstable environments. In a fundamental contribution, Grünig (1984) has demonstrated the influence of the depth over the different phenotypes of Spiroplectammina and Uvigerina in which the forms with spinose ornamentation predominate in deep environments when relatively smooth forms colonized the shallow waters (Fig. 5.9).

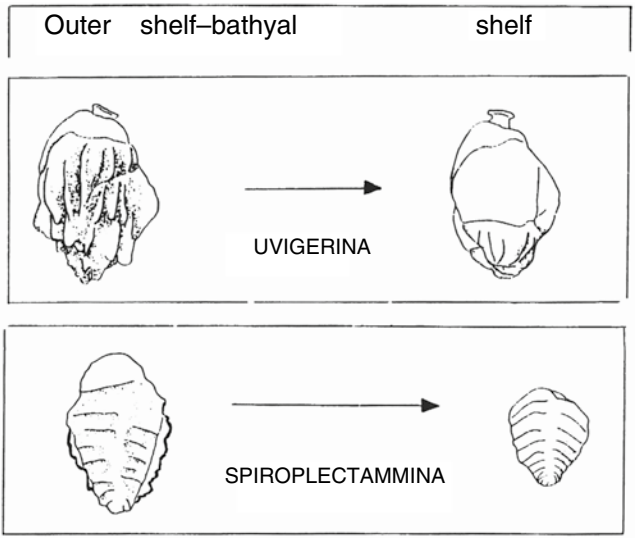

Fig. 5.9 Influence of depth over the different phenotypes of *Spiroplectammina* and *Uvigerina* (From Grünig 1984)

Fig. 5.10 Morphocline showing the extreme forms going from the disorganized glomospiroid type to the typical planispiral *Hemigordius* type in function of environmental stress. Modified from Gargouri and Vachard (1988) in Guex (1992)

On another hand an extreme variability in the Permian porcelaneous foraminifera such as *Hemigordius* (Fig. 5.10) was demonstrated by Gargouri and Vachard (1988) and Mehl and Noe (1990). In this group we observe all the transitions between glomospiroid forms and regular evolute panispiral morphotypes (Fig. 5.10). The glomospiroid morphotypes predominate in the hypersaline waters where nothing else can survive.

5.3.6 Comparison Between the Covariation Observed in Metazoans and Foraminifera

The evolutionary trend observed in the *Ticinella* → *Thalmaninella* lineage discussed in Sect. 3.3 (Fig. 3.2) illustrates the frequent evolutionary trend occurring in coiled shells: in the *T. greenhornensis–T. multiloculata* plexus a strong keel is developed at

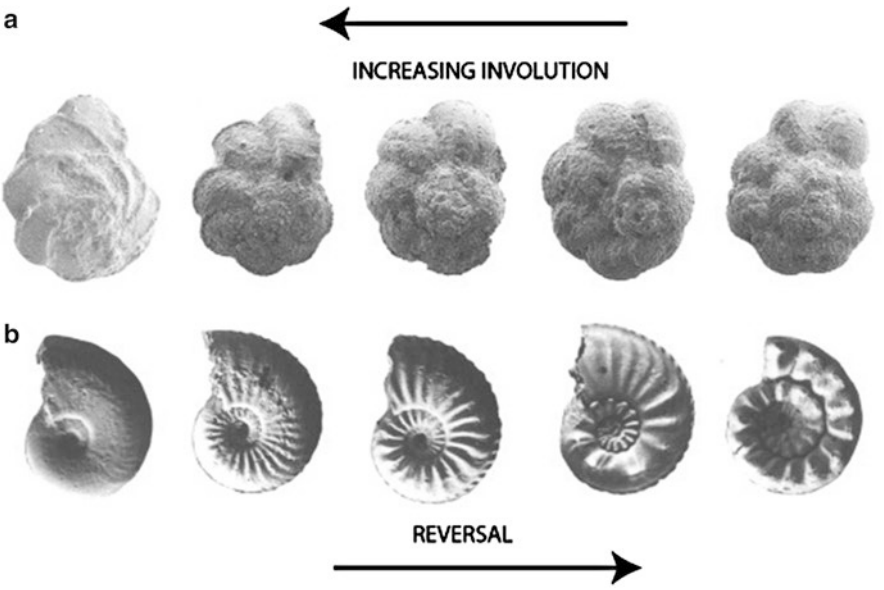

Fig. 5.11 (**a**) Evolutionary lineage going from the simple and evolute ancestral planktonic foraminifera *Ticinella* towards the involute and carinated *Thalmaninella*. (**b**) Highly evolute "*Eoderoceras*-looking" (=ancestral) *Amaltheus* showing a similar trend from evolute towards involute coiling

the maximum lateral curvature of the chamber, demonstrating the relation between morphogen concentration and strong curvature of the membrane. During episodes of environmental stress such as anoxic events, a retrograde polymorphism is observed in these protists, which is perfectly similar to the case of *Amaltheus* described in the preceding section, as illustrated in Fig. 5.11b.

The fact that Buckman's First Law of Covariation applies to both unicellulars and metazoans proves that similar biochemical signals are at work in both types of organisms. This note will be useful for our concluding remarks (see Chap. 9).

5.3.7 Heteromorph Ammonites and Uncoiling of Nautilus *Above the Permian Triassic Boundary*

The contemporary *Nautilus pompilius* is often regarded as one of the most typical example of a living fossil. Indeed, many very old (up to 300 Ma) nautiloids (s.l.) have a shell geometry which is very similar to that of the modern forms. It is therefore surprising to see that this ultraconservative group has been able to behave like ammonoids during major crises (see Fig. 5.12).

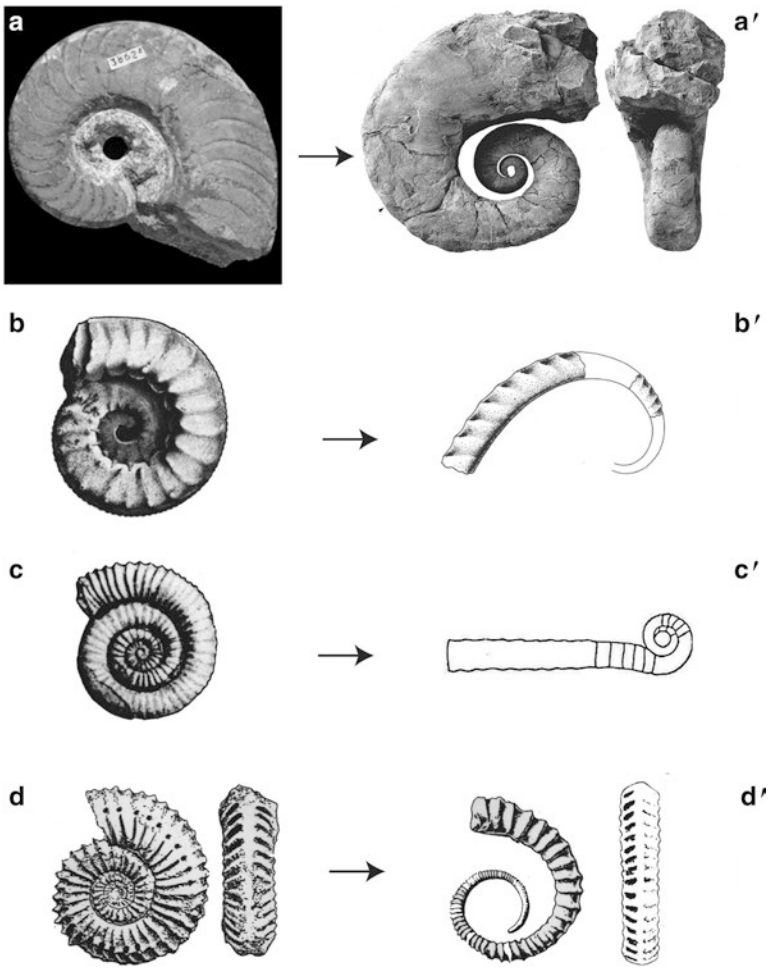

Fig. 5.12 (**a**) *Domatoceras* (Permian), (**a′**) *Gyronautilus* (Early Triassic. From Shigeta 2009), (**b**) *Hybonoticeras* (Tithonian), (**b′**) *Protancyloceras* (Tithonian), (**c**) *Cycloceltites* (U.Norian) (**c′**) *Rhabdoceras* (Rhaetian), (**d**) *Strenoceras* (Bajocian), (**d′**) *Spiroceras* (Bajocian) (**b–d** from Guex 2001)

The unique and fascinating example given here was found by Shigeta (2009) who described an uncoiled nautiloid at the base of the Triassic, deriving from the Pennsylvanian–Permian normally coiled *Domatoceras* (Fig. 5.12A). That extraordinary transition occurred during the catastrophic Permian Triassic transition, which, again, is known to be one of the worst crisis ever occurring on the Earth with 95 % of the species being extinct.

The most spectacular reversals of the trends towards increasing involution are observed among ammonites called "heteromorphs" (uncoiled or with helicoidal coiling) which appear abruptly at various periods of the Triassic and of the Jurassic and which proliferate during the whole Cretaceous.

The oldest uncoiled Mesozoic group belongs to the genus *Rhabdoceras* and derives from the normally coiled *Sympolycyclus/Cycloceltites* group at the base of the Cordilleranus zone, just at the end of a major regressive event. The straight conical *Rhabdoceras* generates semiuncoiled ammonites such as *Choristoceras* (Spath 1933), *Peripleurites* and the helicospiral *Cochloceras*. The Late Triassic heteromorph *Choristoceras* proliferated during the whole Rhaetian when most other typical Triassic ammonoids disappeared. Similar occurrences of uncoiled ammonites are observed during the Middle and Late Jurassic with the appearances of *Spiroceras, Parapatoceras*, discussed below with more detail, and *Protancyloceras*, deriving from normally coiled ammonites.

Magaritz (1989) was one of the first to understand the relationship between some carbon negative shifts ($\delta^{13}C$) and major extinctions in marine faunas. Indeed, it is obvious that collapses of biological productivity occurring during such periods imply massive release of light carbon which, in turn, appears in the stratigraphic record. Taken alone, negative shifts of the $\delta^{13}C$ are not sufficient to deduce the existence of environmental stress but they certainly can be taken as a stress index when they are concomitant with marine regressions and relatively high extinction rates.

In the case of the appearance of *Spiroceras* and *Parapatoceras*, we observe that they are precisely generated during two successive regressive events associated with negative shifts of the $\delta^{13}C$ and clear drops in ammonite diversity (Fig. 5.13). These events could be related to the major changes in the Pacific plates during Middle Jurassic and to the volcanism generated by these events (Bartolini and Larson 2001). The first one appears in the Blagdeni-Banski subzones and derives from lineage *Subcollina* → *Parastrenoceras* → *Strenoceras* which are rooted within more involute Stephanoceratidae. The second one first occurs in the Orbis zone and derives from the lineage *Cadomites* (relatively involute), *Hemigarantiana, Epistrenoceras* (evolute).

Once more this uncoiling is a global process: uncoiled ammonites do not at all resemble juveniles of their ancestors and, therefore, they cannot be considered as "paedomorphs". It is also worth noting that such peculiar groups are perfectly well adapted to the unstable rhaetian and cretaceous environments. For example, one of the only survivor of the End Triassic Extinction (ETE) is *Choristoceras* which survived until the early Hettangian Planorbis zone.

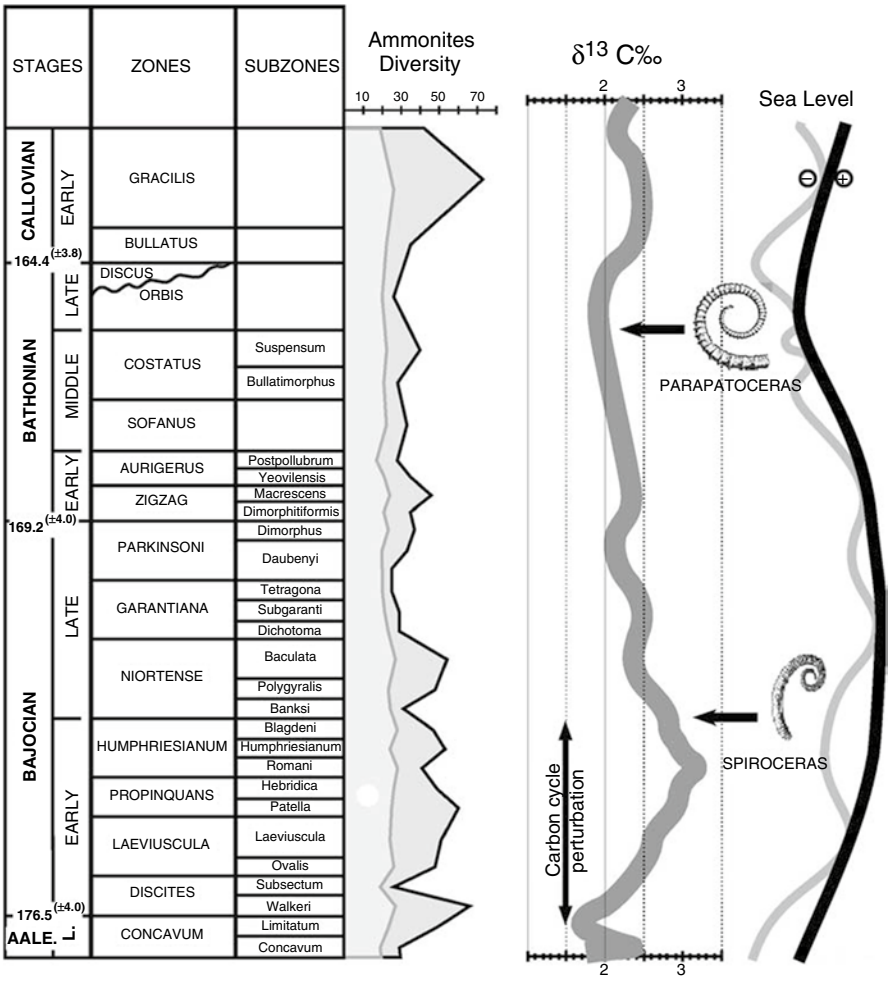

Fig. 5.13 Appearance of the Middle Jurassic *Spiroceras* and *Parapatoceras* during regressive phases and negative anomalies of the $\delta^{13}C$. From O'Dogherty et al. (2006)